

difference, which is an order of magnitude greater than that predicted by  $K$ - $V$  systematics. This unexpected 6% change is greater than the variations in  $K$  observed for the entire compositional range of Mg-Fe solid solution in many oxides and silicates (2).

The observed dependence of  $K$  on Mg-Ti ordering is a consequence of the differential compressibilities of weaker  $\text{Mg}^{2+}\text{-O}$  and stronger  $\text{Ti}^{4+}\text{-O}$  bonds. The structure parallel to the  $b$  axis features an alternating sequence of one M1 and two M2 octahedra. Compressibility along this direction, therefore, is always the average of one Mg-O and two Ti-O bonds, regardless of the state of Mg-Ti order. Compression along the  $a$  and  $c$  axes, by contrast, is dictated primarily by M2 octahedra, which form a continuous edge-sharing octahedral linkage in the (010) plane. In ordered  $\text{MgTi}_2\text{O}_5$ , the M1 (Mg) octahedron is relatively compressible with an octahedral  $K$  of  $172 \pm 4$  GPa, whereas the M2 (Ti) octahedron is relatively rigid with an octahedral  $K$  of  $250 \pm 7$  GPa. In disordered  $\text{MgTi}_2\text{O}_5$ , M1 and M2 octahedra display the same compressibilities, with an average  $K$  of 225 GPa. Crystal compression of this disordered variant is less constrained along the  $a$  and  $c$  axes, and is thus more isotropic.

High pressure has been observed to induce ordering in many silicates (3, 14), including most of the major phases postulated for Earth's mantle (15). This pressure-induced ordering will affect EOS in two ways. First, the typically negative volume of ordering (2) will reduce room-pressure unit-cell volume,  $V_0$ , of mantle phases equilibrated at high pressure; indeed, this negative  $\Delta V_{\text{dis}}$  is the driving force for pressure-induced ordering. Second, ordering will itself affect elastic constants by subtle alteration of compression mechanisms, especially in cases of mixed-valence cation ordering, such as  $\text{MgTi}_2\text{O}_5$ . We conclude that phases with significant  $\Delta V_{\text{dis}}$  greater than 0.1%, including olivines, spinels, pyroxenes, carbonates, and feldspars (2), may also display EOS that are order-dependent.

EOS for geophysically relevant materials are usually made assuming rapid and reversible pressure-temperature-volume systematics. This assumption is invalid for phases that display order-disorder, because  $V_0$ , compressibility, and presumably thermal expansivity are functions of the state of order. Given this situation, seismic velocities alone may be insufficient to resolve compositional effects from those of ordering in some minerals. Determination of EOS of minerals relevant to mantle conditions must thus be performed in situ, on crystals that have ordered states equilibrated with respect to both temperature and pressure.

## REFERENCES AND NOTES

- S. P. Clark Jr., Ed., *Handbook of Physical Constants*, Geol. Soc. Am. Mem. **97** (1966); T. J. Ahrens, Ed., *Mineral Physics and Crystallography: A Handbook of Physical Constants*, Am. Geophys. Union Reference Shelf **2** (1995).
- R. M. Hazen and A. Navrotsky, *Am. Mineral.* **81**, 1021 (1996).
- T. Akamatsu, M. Kumazawa, N. Aikawa, H. Takei, *Phys. Chem. Miner.* **19**, 431 (1993).
- M. C. Domeneghetti, G. M. Molin, V. Tazzoli, *Am. Mineral.* **80**, 253 (1995); R. T. Downs, R. M. Hazen, L. W. Finger, *ibid.* **79**, 1042 (1994); G. Ottonello, A. Della Giusta, G. M. Molin, *ibid.* **74**, 411 (1989).
- C. H. Johansson and J. O. Linde, *Ann. Phys.* **25**, 1 (1936); K. Tsukimura, H. Nakazawa, T. Endo, O. Fukunaga, *Phys. Chem. Miner.* **19**, 203 (1992); H. S. T. O'Neill and W. A. Dollase, *ibid.* **20**, 541 (1994).
- R. M. Hazen, *Carnegie Inst. Washington Yearb.* **80**, 277 (1981).
- T. C. McCormick, R. M. Hazen, N. L. Ross, *Am. Mineral.* **74**, 1287 (1989).
- R. M. Hazen, J. Zhang, J. Ko, *Phys. Chem. Miner.* **17**, 416 (1990).
- R. M. Hazen, *Science* **259**, 206 (1993).
- \_\_\_\_\_, R. T. Downs, L. W. Finger, P. G. Conrad, T. Gasparik, *Phys. Chem. Miner.* **21**, 344 (1994).
- B. A. Wechsler and A. Navrotsky, *J. Solid State Chem.* **55**, 165 (1984); B. A. Wechsler and R. B. Von Dreele, *Acta Crystallogr.* **B45**, 542 (1989); N. E. Brown and A. Navrotsky, *Am. Mineral.* **74**, 902 (1989).
- O. L. Anderson and J. E. Nafe, *J. Geophys. Res.* **70**, 3951 (1965); D. L. Anderson and O. L. Anderson, *ibid.* **75**, 3494 (1970); R. M. Hazen and L. W. Finger, *ibid.* **84**, 6723 (1979).
- Unit-cell parameters and x-ray diffraction intensity data for four crystals were determined at 0.0, 1.03, 2.16, 3.22, 4.34, 6.20, and 7.51 GPa. Unit-cell parameters only were determined at 0.49, 1.68, 2.56, 3.84, 5.12, and 6.95 GPa.
- T. Akamatsu *et al.*, *Phys. Chem. Miner.* **16**, 105 (1988); R. M. Hazen, L. W. Finger, J. Ko, *Am. Mineral.* **77**, 217 (1992); *ibid.* **78**, 1336 (1993); R. M. Hazen, R. T. Downs, L. W. Finger, J. Ko, *ibid.*, p. 1320; R. M. Hazen, R. T. Downs, L. W. Finger, P. G. Conrad, T. Gasparik, *ibid.* **79**, 581 (1994).
- J. Ita and L. Stixrude, *J. Geophys. Res.* **97**, 6849 (1992).
- We thank N. Bector for help in preparation of the samples and C. T. Prewitt and D. Teter for useful discussions and constructive reviews. Crystal chemistry research at the Geophysical Laboratory was supported by NSF grant EAR9218845 and by the Carnegie Institution of Washington. High-pressure studies were supported in part by the NSF Center for High Pressure Research.

29 May 1997; accepted 20 August 1997

## Implications of Satellite OH Observations for Middle Atmospheric $\text{H}_2\text{O}$ and Ozone

M. E. Summers,\* R. R. Conway, D. E. Siskind, M. H. Stevens, D. Offermann, M. Riese, P. Preusse, D. F. Strobel, J. M. Russell III

Satellite observations by the Middle Atmosphere High Resolution Spectrograph Investigation (MAHRSI) have produced global measurements of hydroxyl (OH) in the atmosphere. These observations reveal a sharp peak in OH density near an altitude of 65 to 70 km and are thus consistent with observations from the Halogen Occultation Experiment (HALOE) on the NASA Upper Atmosphere Research Satellite (UARS), which showed an unexplained  $\text{H}_2\text{O}$  layer at the same level. Analysis of stratopause (about 50 kilometers) OH measurements and coincident ozone observations from the Cryogenic Infrared Spectrometers and Telescopes for the Atmosphere (CRISTA) experiment reveals that the catalytic loss of ozone attributable to odd-hydrogen chemistry is less than that predicted with standard chemistry. Thus, the dominant portion of the ozone deficit problem in standard models is a consequence of overestimation of the OH density in the upper stratosphere and lower mesosphere.

The hydroxyl radical is arguably the single most important natural oxidizing agent in Earth's atmosphere (1), yet OH is very difficult to measure because of its high reactivity and thus its extremely low atmospheric abundance. In the middle atmosphere

(between ~15 and 90 km altitude), OH is known to play a fundamental role in the catalytic loss of atmospheric ozone ( $\text{O}_3$ ) (2-4). Although previous ground-based and satellite platforms have produced extensive databases on middle atmospheric  $\text{O}_3$  and  $\text{H}_2\text{O}$  (the parent molecule of OH), the MAHRSI and CRISTA observations have provided the first coincident observations of OH and  $\text{O}_3$  at the stratopause (~50 km) and above (5, 6). In this region, the photochemistry of  $\text{O}_3$  and odd hydrogen ( $\text{H} + \text{OH} + \text{HO}_2$ , denoted by  $\text{HO}_x$ ) is thought to be relatively simple, whereas in the stratosphere  $\text{HO}_x$  chemistry is coupled to other catalytic cycles involving chlorine and ni-

M. E. Summers, R. R. Conway, D. E. Siskind, M. H. Stevens, E. O. Hulburt Center for Space Research, Naval Research Laboratory, Washington, DC 20375, USA.  
D. Offermann, M. Riese, P. Preusse, Physics Department, University of Wuppertal, 42119 Wuppertal, Germany.  
D. F. Strobel, Department of Earth and Planetary Sciences, Johns Hopkins University, Baltimore, MD 21218, USA.

J. M. Russell III, Department of Physics, Hampton University, Hampton, VA 23668, USA.

\*To whom correspondence should be addressed.

trogen species. Although aircraft observations suggest that the current model of  $O_3$  chemistry in the lower stratosphere is reasonably accurate (7), photochemical models of the upper stratosphere and lower mesosphere generally underpredict the  $O_3$  abundance (8). This "ozone deficit" problem, although controversial (9), has persisted despite extensive modeling studies (10), laboratory studies of the kinetics of the  $HO_x$  catalytic system (11), and suggestions of possible additional sources of  $O_3$  production in the atmosphere (12).

The MAHRSI and CRISTA observations, from the German Shuttle Pallet Satellite (ASTRO-SPAS) on the space shuttle Atlantis in November 1994 (6), are well suited for testing  $HO_x$  chemistry in isolation and, in particular, the role of  $HO_x$  chemistry in the ozone budget. The same shuttle mission included the third flight of NASA's Atmospheric Laboratory for Applications and Science (ATLAS-3). The MAHRSI observations consist of limb scans of OH  $A^2\Sigma^+ - X^2\Pi$  solar resonance fluorescence near 309 nm, which are inverted to yield OH density profiles. During 80 orbits of OH measurements, MAHRSI obtained ~1200 daytime limb scans of the OH emission.

The OH density distribution obtained from one representative orbit of MAHRSI observations (Fig. 1A) reflects the two principal photochemical sources of OH. In the upper mesosphere (above ~65 km), OH is produced by photodissociation of  $H_2O$  at ultraviolet wavelengths (principally at the solar hydrogen Ly  $\alpha$  emission line at 121.6 nm). Below ~65 km the dominant source of OH is the reaction  $O(^1D) + H_2O \rightarrow 2OH$ , where  $O(^1D)$  is a product of  $O_3$  photolysis. Because these OH sources depend on the breakup of the water molecule, driven either directly or indirectly by solar radiation, the OH distribution is a function of both  $H_2O$  abundance and solar zenith angle.

The zonal average water vapor distribution for a time period encompassing the MAHRSI mission, obtained from the recently reprocessed HALOE (version 18) observations (13), is shown in Fig. 1B. The morphological similarity between the observed OH and the water vapor distribution in the middle and upper mesosphere (above ~60 km) is striking and is a consequence of the large sensitivity of OH to  $H_2O$  in this region (14). In the early morning, when the solar zenith angle is high, the contours portray the formation of OH after sunrise. As the solar zenith angle decreases below ~60°, the OH data begin to reflect the ~25% variation in the latitudinal distribution of  $H_2O$ . In the lower mesosphere (~50 to 60 km altitude), where photolysis of  $O_3$  indirectly controls the OH source, both  $O_3$  and  $H_2O$  exhibit little diurnal variation.

Furthermore, the OH and  $O_3$  densities here are expected to have weak dependences on the water vapor abundance, that is,  $[O_3] \propto [H_2O]^{-1/3}$  and  $[OH] \propto [H_2O]^{1/2}$  (4). Because the  $H_2O$  abundance in the lower mesosphere varies by less than ~10% between 50°S and 50°N, latitudinal variation in water vapor contributes little to the variation in OH and  $O_3$ . The OH density below ~60 km is therefore primarily dependent on the solar zenith angle, which is a slowly varying function during the day, as seen in the OH observations in Fig. 1A.

The retrieved OH density profiles from 18 orbits of observations on 5 and 6 November 1994 that were within  $\pm 5^\circ$  of latitude of 30°S, 10°N, and 35°N are shown in Fig. 2. These latitudes were chosen to test

model  $HO_x$  chemistry under early-, mid-, and late-morning solar illumination conditions. For each latitude bin, the data from all orbits show remarkable coherency, comparable to the estimated measurement random error (6, 15).

We used a one-dimensional, time-dependent photochemical model to simulate the diurnal variation of OH and  $O_3$  (14). Because  $H_2O$  is long-lived (with a chemical lifetime of weeks to months), we fixed model water vapor abundances to the HALOE values. Results for three model cases are shown along with the MAHRSI OH data in Fig. 2. In model A, we assumed standard  $HO_x$  chemistry, denoted here by JPL94 (11). In model B, we assumed a 50% reduction for the rate coefficient for

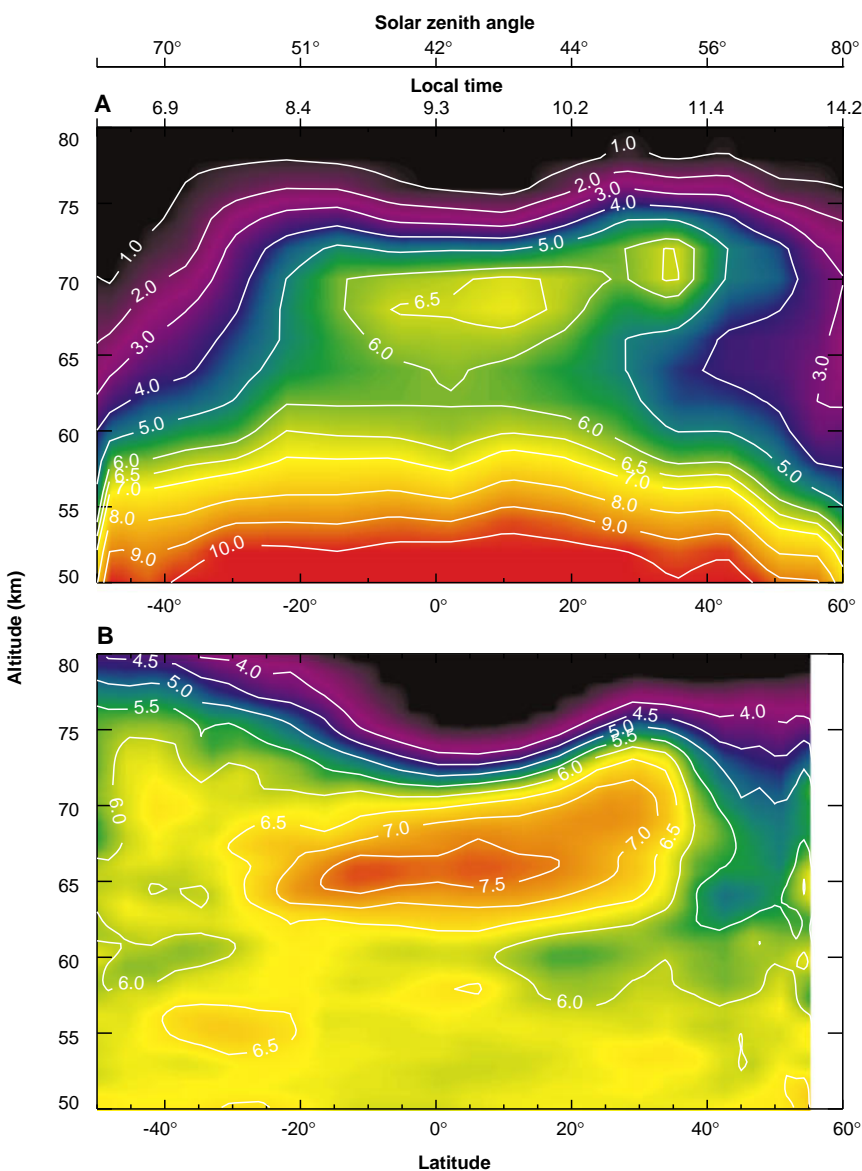


**Fig. 1.** (A) Retrieved MAHRSI OH number density (units of  $10^6 \text{ cm}^{-3}$ ) as a function of altitude and latitude for MAHRSI orbit 27 on 5 November 1994. The solar zenith angle and local solar time of the observations are indicated at the top. (B) Zonal average  $H_2O$  mixing ratio (parts per million by volume) generated by plotting daily average HALOE sunrise occultation profiles for 23 October to 30 November 1994.



In model C, we assumed a 20% reduction in the rate coefficient for reaction 1 along with a 30% increase in the rate coefficient for



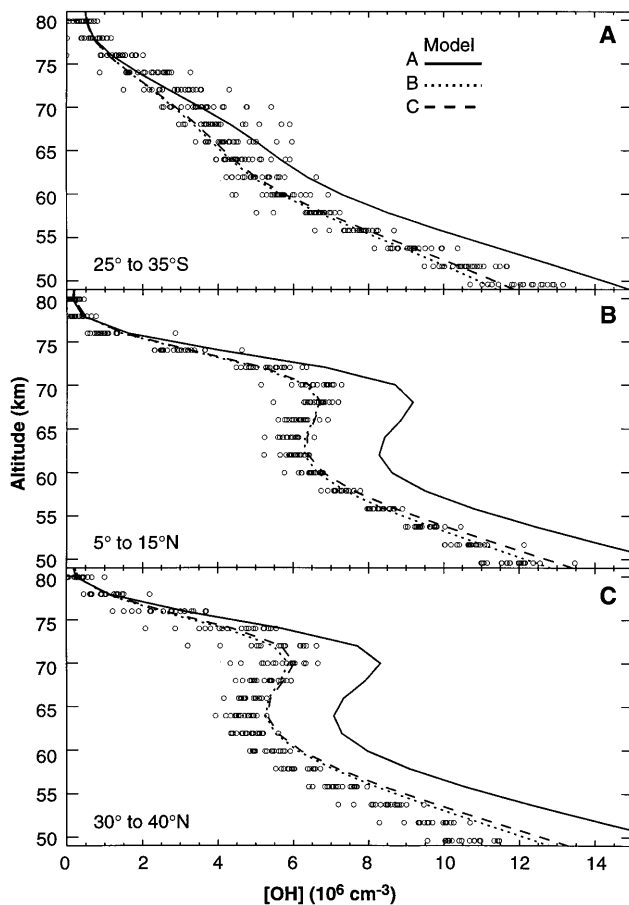
Model B arises from a study of ground-based microwave observations of HO<sub>2</sub> and O<sub>3</sub> by Clancy *et al.* (16), who proposed a major reduction of ~50 to 70% in the rate coefficient for reaction 1 so as to bring theory into acceptable agreement with their observations of both of these species in the lower mesosphere. This is 2.5 to 3.5 times the quoted measurement uncertainty in JPL94. The modifications for model C are equivalent to the estimated 1σ measurement uncertainty (11) for both of these reactions. A decrease in the rate of reaction 1 decreases the OH/HO<sub>2</sub> ratio, whereas an increase in the rate of reaction 2 decreases total HO<sub>x</sub>.

Standard HO<sub>x</sub> chemistry overestimates the OH abundances below ~75 km altitude for the 10°N and 35°N latitudes, and below ~65 km for 30°S. However, models B and C both give good agreement at all three latitudes and all altitudes, with the exception of a region centered at ~70 km

for 30°S (where there is a slight underprediction). The agreement near the OH peak at ~65 to 70 km is largely a consequence of the high peak H<sub>2</sub>O mixing ratio at that level seen in the version 18 HALOE H<sub>2</sub>O profiles. Models of OH using earlier (version 17) HALOE H<sub>2</sub>O profiles do not agree with the MAHRSI OH data, because those H<sub>2</sub>O data did not show such a pronounced maximum near 65 to 70 km (14, 17).

Near the stratopause (~50 km), the model OH with standard HO<sub>x</sub> chemistry overpredicts the observed values by ~30 to 40%, as previously shown (14). Of the three latitude bins, the best agreement between model OH and observed profiles is at 10°N, where HALOE H<sub>2</sub>O observations were obtained on 7 November 1994, only 1 to 2 days after the MAHRSI observations. Middle atmospheric H<sub>2</sub>O undergoes a slow seasonal cycle in response to the changing circulation and solar insolation. Hence, only a slight change in H<sub>2</sub>O would be expected to occur in a 2-day time period. Because of the latitudinal precession of the HALOE occultations, the models use HALOE H<sub>2</sub>O data from sunrise occultations that were made on 15 November and 1 November 1994, respectively, for 30°S and 35°N.

**Fig. 2.** Retrieved MAHRSI OH density profiles from 18 orbits of observations during 5 and 6 November 1994, within three latitude ranges: (A) 25° to 35°S, (B) 5° to 15°N, and (C) 30° to 40°N. The photochemical model results at the mean latitudes and at the appropriate local solar times were convolved with the MAHRSI weighting functions. Results are shown for the three models discussed in the text; models B and C are nearly indistinguishable.



The effects of modified HO<sub>x</sub> chemistry on the OH and HO<sub>2</sub> density profiles are shown in Fig. 3. Model B leads to a change of less than 10% in the calculated OH and HO<sub>2</sub> density profiles below 30 km altitude. Thus, this model would have little impact on lower stratospheric (≤30 km) chemistry (7). Near 40 km altitude, model B yields an OH density ~25% lower than standard chemistry; this appears to be consistent with recent studies of in situ balloon measurements (18), which showed that standard chemistry overestimates OH by 20% at 37 km (near the highest altitude of the balloon measurements). Model C leads to larger changes in both OH and HO<sub>2</sub> in the lower stratosphere, which are probably incompatible with the balloon measurements. In the mesosphere, both modified HO<sub>x</sub> models lead to somewhat similar decreases for OH density, but the results for HO<sub>2</sub> are distinctly different. Model B leads to relatively large increases in HO<sub>2</sub>, whereas model C yields a much smaller increase. Ground-based observations of high values of HO<sub>2</sub> in the lower mesosphere (16) favor model B.

These modifications to HO<sub>x</sub> chemistry, which appear to be necessary to explain the MAHRSI data, have important consequences for the ozone budget. At the stratopause and above, ozone loss is dominated by HO<sub>x</sub> catalytic cycles (3). A critical test of the validity of lowered HO<sub>x</sub> catalytic loss rates on O<sub>3</sub> can be made by a direct comparison between models and coincident OH and O<sub>3</sub> observations.

Coincident MAHRSI OH and CRISTA O<sub>3</sub> observations at 50 km altitude for orbit 27 (19) are shown in Fig. 4. The large-scale variations with latitude in the CRISTA O<sub>3</sub> data are thought to be real, because they are seen in a similar way by the two lateral telescopes of the CRISTA instrument (20). Shown along with the CRISTA O<sub>3</sub> data in Fig. 4B are O<sub>3</sub> mixing ratios obtained from HALOE observations

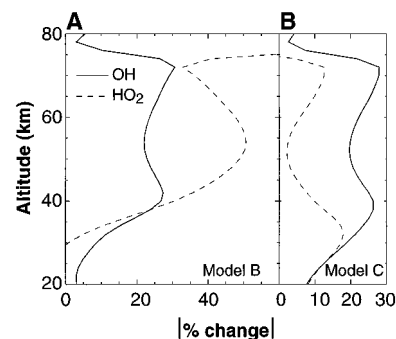


**Fig. 3.** Percentage change in model OH and HO<sub>2</sub> densities (A) between standard HO<sub>x</sub> chemistry and model B, and (B) between standard HO<sub>x</sub> chemistry and model C.

on the same day as the MAHRSI and CRISTA observations. On this day HALOE sampled latitudes from  $\sim 9^\circ$  to  $19^\circ\text{N}$ , and the zonal mean  $\text{O}_3$  mixing ratio obtained from both sunrise and sunset occultations was  $\sim 2.5$  parts per million by volume (ppmv) (21). The Millimeter-wave Atmospheric Sounder (MAS) on the ATLAS-3 mission also observed  $\text{O}_3$  on 4 November 1994; the inferred  $\text{O}_3$  mixing ratios from MAS nearest to the HALOE and CRISTA measurements are also shown. The three separate ozone measurements are in general agreement.

Also shown in Fig. 4 are results from a set of photochemical model runs at five locations along the orbit at the appropriate local solar times of the observations. The standard model shows a clear OH overprediction at all latitudes along with an underprediction of  $\text{O}_3$ ; this is an illustration of the ozone deficit problem in standard models. Lowering model OH by the above  $\text{HO}_x$  modifications leads to larger values of  $\text{O}_3$  (less  $\text{HO}_x$  catalytic destruction of active oxygen). Both modified  $\text{HO}_x$  models lead to better agreement with

the CRISTA  $\text{O}_3$  data. Standard chemistry produces  $\sim 20$  to 25% less  $\text{O}_3$  than the modified  $\text{HO}_x$  models. Thus, the dominant component of the ozone deficit is attributable to the standard chemistry overestimate of OH. This is no surprise, because suggestions to that effect were made as early as 1985 (22). The difficult nature of remote satellite measurements of OH long delayed this experimental confirmation of the earlier suggestions.

Our results show that the MAHRSI OH and HALOE  $\text{H}_2\text{O}$  data provide a consistent picture of the odd-hydrogen photochemistry in the mesosphere. A 5-year climatology of HALOE water vapor observations (23) at low latitudes shows a peak in the  $\text{H}_2\text{O}$  mixing ratio near 50 km, a slight decrease just above this level to a minimum near  $\sim 60$  km, and an increase to a secondary maximum near 65 to 70 km. This second peak in the HALOE  $\text{H}_2\text{O}$  data (Fig. 1B) is essential to agreement between the model OH and the data, and thus the MAHRSI OH observations indirectly support the existence of this feature in the HALOE data. However, this second peak is not seen in long-term ground-based observations (24)—likely because of the much lower vertical resolution (7 to 10 km) of the ground-based technique—nor in two-dimensional models of mesospheric water vapor (25). Furthermore, the observed peak value of  $\sim 8$  ppmv of  $\text{H}_2\text{O}$  as seen by HALOE near the equator (Fig. 1B) represents a violation of “total hydrogen”—that is,  $2 \times \text{CH}_4 + \text{H}_2\text{O}$ —which is observed to be less than  $\sim 7$  ppmv in the lower stratosphere (25). As a result, this observed double-layer  $\text{H}_2\text{O}$  mixing ratio distribution brings into question our basic understanding of the sources and sinks of middle atmospheric water vapor (23).

These MAHRSI OH observations have implications for other aspects of middle atmospheric chemistry, such as CO loss (26),  $\text{H}_2\text{O}$  photochemical recycling (3),  $\text{CH}_4$  oxidation (25), and release of active chlorine through  $\text{OH} + \text{HCl} \rightarrow \text{Cl} + \text{H}_2\text{O}$  in the upper stratosphere. For example, the standard model overprediction of OH in the upper stratosphere may provide an explanation for the overprediction of ClO in this region (27). Our study reveals the need for (i) further coincident OH and  $\text{O}_3$  observations, particularly for different seasons; (ii) independent observational verification of the middle mesospheric  $\text{H}_2\text{O}$  peak seen by HALOE; (iii) a reevaluation of the laboratory determinations of  $\text{HO}_x$  chemical rate coefficients that dominate mesospheric ozone loss; and (iv) increased emphasis on measurements of  $\text{HO}_2$  in the upper stratosphere and low-

er mesosphere, because OH- $\text{HO}_2$  partitioning is a key test of proposed  $\text{HO}_x$  chemistry modifications.

## REFERENCES AND NOTES

1. A. M. Thompson, *Science* **256**, 1157 (1992).
2. D. R. Bates and M. Nicolet, *J. Geophys. Res.* **55**, 301 (1950).
3. G. Brasseur and S. Solomon, *Aeronomy of the Middle Atmosphere* (Reidel, Dordrecht, Netherlands, 1984).
4. M. Allen, J. I. Lunine, Y. L. Yung, *J. Geophys. Res.* **89**, 4841 (1984).
5. D. Offermann and R. Conway, *Eos* **76**, 337 (1995).
6. R. R. Conway *et al.*, *Geophys. Res. Lett.* **23**, 2093 (1996).
7. R. C. Cohen *et al.*, *ibid.* **21**, 2539 (1994).
8. D. E. Siskind *et al.*, *J. Geophys. Res.* **100**, 11191 (1995).
9. P. J. Crutzen, J.-U. Grob, C. Brühl, R. Müller, J. M. Russell III, *Science* **268**, 705 (1995).
10. R. T. Clancy *et al.*, *J. Geophys. Res.* **92**, 3067 (1987); D. F. Strobel *et al.*, *ibid.*, p. 6691; J. Eluszkiewicz and M. Allen, *ibid.* **98**, 1069 (1993).
11. W. B. DeMore *et al.*, *Chemical Kinetics and Photochemical Data for Use in Stratospheric Modeling* (Publ. 94-26, Jet Propulsion Laboratory, Pasadena, CA, 1994).
12. R. L. Miller *et al.*, *Science* **265**, 1831 (1994); J. M. Price *et al.*, *Chem. Phys.* **175**, 83 (1993); T. G. Slanger, L. E. Jusinski, G. Black, G. E. Gadd, *Science* **241**, 945 (1988).
13. J. M. Russell III *et al.*, *J. Geophys. Res.* **98**, 10777 (1993).
14. M. E. Summers *et al.*, *Geophys. Res. Lett.* **23**, 2097 (1996).
15. The systematic errors for the MAHRSI OH observations are estimated to be +23%, -20%.
16. R. T. Clancy, B. J. Sandor, D. W. Rusch, *J. Geophys. Res.* **99**, 5465 (1994).
17. The HALOE team has done extensive checks on the version 18 data to determine the effects of data smoothing, transmission calculation errors, and other more subtle factors on the high-altitude feature, and they have found no reason to question their reality.
18. G. B. Osterman *et al.*, *Geophys. Res. Lett.* **24**, 1107 (1997).
19. We chose the 50 km altitude for the stratopause analysis because the retrieved OH densities become increasingly sensitive to background subtraction and the estimated uncertainty increases substantially below that level. Also, the CRISTA  $\text{O}_3$  observations above  $\sim 55$  km begin to be influenced by non-LTE (non-local thermodynamic equilibrium) effects, and the observations at 50 km altitude are currently near the highest altitude at which non-LTE effects can be safely ignored in the retrievals.
20. For improved horizontal coverage, CRISTA uses three telescopes directed at  $180^\circ$ ,  $162^\circ$ , and  $144^\circ$  with respect to the velocity vector (5). The absolute errors of the CRISTA  $\text{O}_3$  data are estimated to be 15 to 20% at the present stage of data evaluation, whereas the precision of the data is estimated to be better than  $\pm 3\%$ .
21. The HALOE estimated random plus systematic error for  $\text{O}_3$  is 8% or  $\sim 0.2$  ppmv.
22. D. W. Rusch and R. S. Eckman, *J. Geophys. Res.* **90**, 12991 (1985).
23. D. E. Siskind *et al.*, in preparation.
24. G. E. Nedoluha *et al.*, *J. Geophys. Res.* **100**, 2927 (1995).
25. M. E. Summers *et al.*, *ibid.* **102**, 3503 (1997).
26. S. Solomon *et al.*, *J. Atmos. Sci.* **42**, 1072 (1985).
27. A. E. Dessler *et al.*, *Geophys. Res. Lett.* **23**, 339 (1996).
28. We thank NASA for providing UARS Guest Investigator funding and C. Aellig for providing the MAS data. Supported in part by the Office of Naval Research and by the Atmospheric Remote Sensing and Assessment Project of the Strategic Environmental Research and Development Program.

23 June 1997; accepted 4 August 1997

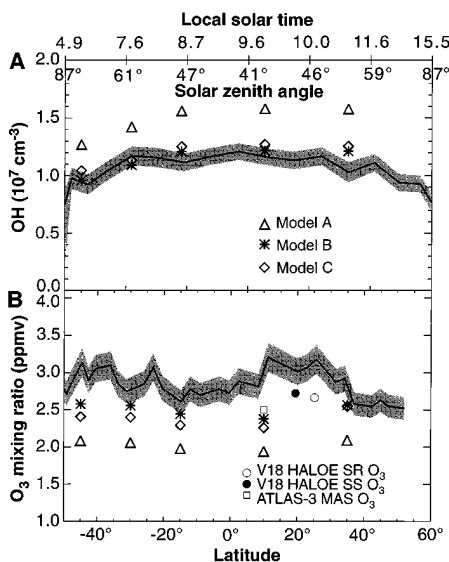


**Fig. 4.** (A) Retrieved MAHRSI OH number densities at 50 km altitude for orbit 27 on 5 November 1994. The local solar time and solar zenith angle at the tangent point are indicated at the top. The shaded area shows the estimated MAHRSI OH random measurement error propagated through the retrieval. (B) Ozone mixing ratio inferred from coincident CRISTA observations for the same orbit. The shaded area represents a  $3\sigma$  range, where the  $1\sigma$  measurement error is estimated to be  $\pm 3\%$  in the retrieved mixing ratio. UARS HALOE sunrise (SR) and sunset (SS)  $\text{O}_3$  and ATLAS-3 MAS  $\text{O}_3$  mixing ratios for the same day closest to the MAHRSI and CRISTA observations are shown. In both panels, results are shown at the appropriate local times and latitudes for the three models discussed in the text. Model OH was convolved with the MAHRSI weighting functions.